Wireless Networks (2025) 31:2925–2938
https://doi.org/10.1007/s11276-025-03923-5

ORIGINAL PAPER

A novel compact flower shaped antenna array for sub-6 GHZ and UWB applications

G. Santhakumar[1] · R. Muthukumar[2]

Accepted: 3 February 2025 / Published online: 19 February 2025

Abstract
The demand of high-speed data rate transfer, streaming and the expansion of the infrastructure of the Ultra-Wide Band communication in means of wireless communication has become a vital consideration in improving the Gigabits bitrate. The usage of MIMO antenna in many wireless applications acts as both the source of transmitter and receiver. These antennas are advantageous in working with higher rate of data, diverse time and with diverse frequency range. The proposed study utilize the two-element flower shaped Ultra-Wide Band Multiple Input Multiple Output (MIMO) antenna with a dual notching of range 5.6 GHz and 7.2 GHz which comprises good isolation rate.The antenna uses a dodecagon shaped Complementary Split Ring Resonator (CSRR) for the realization of notching with range of 7.2 GHz. A novel decoupled structure is used for enhancing the rate of isolation loss. The substrate RT Duroid 5880 is used with a dielectric constant at a range of 2.2 and a height (length) of 0.79. The complete size of the antenna ranges from $30.5 \times 42.2 \times 0.79$ mm^3. The S_{11} is obtained less than -10 dB by using the antenna. The range of VSWR is less than 2. The isolation loss is at a considerable range constituting the entire band. The complete bandwidth of the proposed antenna is in a measurable range. The antenna's performance is evaluated based on parameters such as Total Active Reflection Coefficient, Channel Capacity Loss, Diversity Gain, Mean Effective Gain, and Envelope Correlation Coefficient.

Keywords Ultra wide band-multiple input multiple output antenna · Stub · Resonator · Wireless network systems · Impedance bandwidth

1 Introduction

The demand of wireless communication grows widely over few decades. The new paradigm of wireless communication are the 6G systems, which operates using the AI techniques, which is adapted to operation in year of 2027–2030 [1]. The rapid growth of smart devices and Internet of Everything (IoE) in a situation requires more data, which is ultra-reliable and low-latency in the phase of communication. These serve as a key technology for serving the emerging trends and future networks [2]. The tactile internet and multi-sense experience are in the line of digital win, where the capabilities of the network such as holographic-type communication are using ubiquitous intelligence, in need of showing excellence in research activities and specifications [3]. A stable and a proper configured network communication, for an enhanced speed of network connectivity is needed.

The deployment in the 5G systems are exposed in the inherent limitations of system, which is compared to the original premise and is enabled for IoE applications [4]. The evolution of wireless network drives the primary need at higher rates [5]. These are mandatory at a higher rate of increase, in networking capacity. This connect billions of people, using the enhanced mobile broadband services [6]. The wireless communication and their technologies are continuously developed in order to meet the advanced needs from the 1st generation to the 5G, wireless communications which are commercially available on a large platform [7]. The lack of control over the wireless channel and increased power consumption are some of the limitations, which are associated with the wireless technologies and interface [8].

✉ G. Santhakumar
g.santhakumarece@gmail.com

R. Muthukumar
muthukumarr2004@gmail.com

[1] Department of ECE, Sri Krishna College of Technology, Coimbatore, India

[2] Department of EEE, Erode Sengunthar Engineering College, Erode, India

To reduce these issues, configuration techniques is used for making green and sustainable future in the cellular form of networks using the Intelligent Reflecting Surfaces [9].

These wireless networks should be adapted to use them with the high quality of experience and with a reliable connectivity [10]. These 6G communications face more challenges in supporting the extensive varieties, which are more prone to face heterogeneous traffic, and satisfying the service-quality related parameters [11]. The optical form of wireless communication with the other associated wireless communications, serve as a promising and effective solution for the successful deployment of wireless networks in IoT systems [12]. The Terahertz link play a major role in the high level of data rate communication at fewer distance range. To achieve task, [13] the antennas are constructed with high gain and wideband characteristics which suits the THz communication technologies. Recently, the need for smaller size antennas are expanded in stabilizing the wireless communications. These methods scrutinize the effect of dielectric super states, on various parameters [14]. The adaption of MIMO antennas for wireless form of communications are made to adapt the advancements by making both the transmitter and receiver independent [15].

The UWB- MIMO (Ultra Wide Band Multiple Input Multiple Output) antennas uses in case of the wireless technologies and communications. These are connected to dual notching point, which are at a range of 5.6 GHz and the 7.2 GHz. These are incorporated with a proper and good isolation technique. The band-notched UWB antenna is used for switching between the two notch bands, it can be used in tuning the central frequency. To fulfill the demands of frameworks of the IoT and developed mobile applications, which have become smaller and more compact mean of communication [16], Dielectric Resonator Antenna uses. These approached antennas provides many advantages such as compact size, high efficacy, and wide-band behavior [17]. The upper edge of the common ground is stepped and incorporated with plus shaped slotted stubs in view of enhancing the isolation among the elements of antenna, the stubs uses as a band stop filter at a desired range of frequency [18].

The substrate is used in the antenna is provided for the mechanical support to the antenna, which consists of dielectric material, which is fabricated using technologies [19]. Dielectric substrates uses in creating a separation, among the two metal surfaces, in order to facilitate the electric field generation [20]. A substrate RT duroid 5880 with a dielectric constant range of 2.2, and height of 0.79. A U-shaped slot is utilized, which is attached to the patch, to center the notching band at 7.2 GHz. In order to prevent the return loss used in depicting the efficiency of antenna, by improving the impedance bandwidth and the return loss. The value of S_{11} indicates the measure of power, which is reflected in the port of antenna due to some mismatch from the line of transmission, and not received by the antenna [21]. The complete size of the antenna remains in the range of $30.5 \times 42.2 \text{x} 0.79$ mm^3. The return loss (s_{11}) obtained from the antenna is less than -10 dB.Whereas conversely, the isolation loss is more than -20 dB, on the entire band. There are some chances that leads to an antenna mismatch, which is indicated using the Voltage Standing Wave Ratio (VSWR) [22]. This indicates the mismatch among the antenna with the feed line, which is connected to it which range from a value of 1 to ∞ [23]. The suggested model achieves a VSWR at a range of 2. The complete bandwidth of antenna is achieved at a range of 3.1–14 GHz. The suggested model is evaluated for its performance with Active Reflection Coefficient, Mean Effective Gain (MEG) and the Channel Capacity Loss (CCL). The suggested antenna is simulated using the HFSS software, High Frequency Structure Simulator, one of a well established and a fine element method which involves numerous features, in designing the parametric geometry modelling and in optimization algorithms [24].

1.1 Aim and objective

The main aim of the research relies in implementing the antenna using enhanced data rate capacity and fulfilling the wider bandwidth range with improved capacity and speed in modern communication.

- To implement the MIMO antenna with the UWB, for enhanced capacity of bandwidth.
- To prevent the isolation loss using the appropriate substrate and resonator implementation.
- To evaluate the proposed method using the appropriate metrics calculation and metrics method.

1.2 Paper organization

Section 1 describes a brief introduction about the entire methodology covered in the study. Section 2 depicts some of the existing methods and methodologies along with their limitations. Section 3 represents the proposed methodology with a complete flow diagram. Section 4 discusses about the experimental outcomes of the proposed research. Section 5 delivers a short and an overall conclusion about the entire work and methods carried out in the study.

2 Review on existing methods

The suggested study, uses a [25] UWB, which are more prompt in the wireless form of communication, and an micro-strip antenna, a monopole antenna over a plate and also a meta-material and a flexible UWB antenna. These are devoid in developing the delicate transistors, connectors

and the flexible feeding lines, needed to has incorporated with the GND layers, and can be made use in the e-textiles. To enhance the carrier frequencies, from the mm range to the THz, are a potential solution [26], by enhancing the transmission rate and also the channel capacity. These can be associated using the Fabry–Perot Cavity theory used in the manufacture of AM technology, which is more reliable, and are at low-cost. The advanced antenna design are constructed using the micro-strip antenna which has lower profile and a simple manufacturing means, and are also ease to feed. But the total efficiency of the antenna remains in the range of − 3.116 dB [27]. The micro-strip antenna has been simulated using the HFSS EM simulation software. These uses in the WiMAX and in the WLAN. These had achieved an return loss of − 30 dB with 1.2 VSRW [28].

A hexa-band frequency, which is reconfigurable with a wide range of tuning band, has used by connecting and re fabricated to the PIN diode. But the return loss of these antenna are in a range of − 10 dB and with a single band node of − 26.81 dB [29]. A jug shaped UWB [30], which are printed using a low-cost FR substrate, with a loss tangent of 0.025, which are less suitable for the wireless communication systems. The measured reflection coefficient and the obtained radiation pattern are at a close agreement, and the overall efficiency of the antenna is 85% in the entire band [30]. The compact slotted antenna, which has patterned on a FR4 substrate, which has a dielectric constant material of 4.4 and a loss value of 0.008. this suggested study has a gain value of 1.07 to 3.92dBi [31].

A co-planar wave-guide antenna with a circular monopole is used with an increased impedance, which has a greater frequency range more than 20 GHz, but the performance of the antenna depends on the width of ground plane and with the feed gap along with the dimensional risk [32]. The CNT (Carbon Nanotube Antenna) which uses as the antenna in the wireless communications had indicated that their performance couldn't match with the metals such as copper. But these cannot match up the radiation levels efficiency [33]. A compact stair-shaped antenna has used in the wireless communication systems, which uses in the evaluation of operating bands and in the characteristics of radiation. These are fabricated using the FR-4, showed good segment but lagged in some of the cases due to the soldering effects, small dimension in the fabrications and also due to the use of anechoic chamber used in the measurement resulting in leakage of the sources and leading to deflections [34]. A high-gain tampered slot antenna has used for the purpose of underwater communication, in a microwave band, which are fabricated using the FR-4 epoxy substrate material, with a dielectric value of 4.4 and tangent loss value of 0.02. These can achieve a impedance bandwidth above 55% and with a 10 dB loss value, and of a 90% in accuracy rates [35]. The low-profile multi-slotted antenna has tailored using a steeped rectangular form of radiating element, which has been printed on both of the sides using a FR4 substrate. These had attained a good efficiency and also exhibits an omnidirectional pattern making more suitable for the 5G applications, while the operating bands are at a range of 3.15–5.55 GHz [36]. This study [37] multi-band bowtie slot antenna is used as a compact and also with a high gain properties, having an antenna structure and with a copper conducting sheet which are chambered to the ground plane. These exhibit a high gain value of 6.3 dBi at all of the varying resonances. The dual band eight-array antenna is used in 5G mobile terminals. The required dual-resonance is obtained by the adjusting the SIR impedance ratio, and by tuning the position of feed line of the micro strip. The return loss of these antenna are 10 dB, and the efficiency values are about 51% [38].

The circularly polarized antenna along with a non-uniform meta-material reflector is used which had a modified and a wide s-shaped slot antenna with a NUM reflector. These are end with a triangular patch in order to remove the axial ratio, and the impedance bandwidth. The reflector used here are unevenly distributed, the peak-gain values of 6.0dBi are obtained by using a 3.8GHZ, reflector [39]. In this suggested study [40], the circularly polarized antenna (CP) which is based on the zero-index material is used along with a square ting, having two asymmetrical split is used as a unit cell for achieving a high gain value and also an circular polarization. This has achieved using the optimization of two-split gaps on the ring present in the unit cell and has been verified experimentally, which showed an impedance bandwidth of 7.04 to 7.68 GHz. In this study [41], a low-profile broadband with a polarized antenna with a single-layered meta-surface fi designed which composes 4 × 4 rectangular loops which are rotated. Instead of using a single rotted rectangle, an inner-cut rectangle can be using in enhancing the flexibilities and by changing the slot size. These can also be achieved by the process of reducing the size of antenna, ranging in the impedance bandwidth of 5–6.05 GHz.

The low-profile CP antenna with a wideband along with the polarization–reconfigurable characteristics has used in the study, which has an antenna with truncated-corners works as a CP and with a non-uniform meta-surface. These can act as a parasitic element for the enhancement of the performance. These uses in producing additional operating bands with a higher frequency rates and are combined with the lower bands, to broaden the operating bandwidth. These shoed an impedance range of − 10 dB, and with an axial ratio of 25.6% [42]. Wave tampered slot antenna is used with a compact size, used in the wireless communication, which is developed using a roger duroid 5880, with a working range of 6 GHz–21 GHz. The opening taper profile and the radial cavity are maintained using the simple feeding technique [43]. A multi-stored patch antenna uses in wide operating band which is achieved by good coupling techniques, among

the radiator and the ground, these can help in reducing the slot size of the antenna, with a dependency and also using the undesired cross-polarization fields. These are suitable in making portable communications and can exhibit a Omni-directional radiation pattern with a $S_{11} \leq -10$ dB [44].

For the applications of base-stations, a triple band, which are dual polarized and are multi slotted antenna uses especially for 5G base stations. These has been designed to cover, two bands from n77 and one more from n79 5G NR frequency spectrum. These are with higher isolation and with a cross-polarization ratio of which discrimination, which resulted in a measured gain of 16.65 dBi and 15 dB of return loss [45]. In this suggested study, a π-shaped micro-strip patch antenna has used with a partial ground structure for 5G WiMAX application and for the WiFi applications. These are optimized using the Computer simulation technology, and with microwave studio, mounted with roger RT5880 with a Relative Permittivity value of 2.2. These are more suitable for the lower 5G, WiFi and also for the WiMAX communication application also [46]. For the implementation of future 5G mm wavebands, the Multi-slotted antenna in array size, which are more compact and has been used for the wireless 5G communications, with higher frequency range and at moderate bandwidth rate. The maximum gain value are at 3 dB and the bandwidth range are at 200 MHz to 700 MHz [47].

A reconfigurable form of 2×2 UWB MIMO antenna is use in with the same plane and with an orthogonal plane uses m many such applications such as imaging and in the applications of imaging. This antenna [48] is made use of the FR-4 substrate, which is of a thickness about 0.8 mm and with a coplanar waveguide feeding mechanism. The two-pin diode, which uses to patch resulting in, enhanced re-configurability of the antenna. These can also restrict the WiFi and the WiMAX signals. This antenna provides a complete bandwidth with a range of 87–90%. The rejection of the interfering bands along with the operating bans are intended for the UWB-X band applications which uses a diversified antenna with a complete dimension range of $24 \times 48 mm^2$. These has obtained using the anchor-shaped stub, which is embedded into the slotted radiating patch, used in offering an enhanced isolation rate more than 30 dB, in both the simulated and in the measured environments. These antennas are capable of offering various S-parameters, efficiency in radiation and various radiation patterns [49].

The four-port notched band with the MIMO are investigated using the fabricating prototype [50]. These are initially prototyped with the 2×2 MIMO configuration and then with the 4×4 MIMO configuration. These antenna offers a ECC in a range of < 0.02, and a TARC in a range of ≤ 20 dB and an overall efficacy rate of 80% along with a stable pattern of radiation. The isolation-enhanced low profile MIMO uses along with the dual-band notched features uses in the antenna, which possesses a staircase like radiators for achieving an enhanced bandwidth rate. These elements, which are radiated, are perpendicular, in order to achieve enhanced polarization and with high isolation loss rate. The CSRR, is used in the suggested antenna which achieves the S_{21} range more than -20 dB [51]. The enhanced and better mutual coupling rates has achieved using the appropriate decoupling structures, which in turn reduces the entire complexity of the system. This suggested antenna offers a gain value in a range of 0.787, which are less suitable for a wireless working system. This antenna had a hexagonal shape with a two spherical shaped structures in the corner. The patch to the respective antenna using the inverted T and C slots in order to block both the WiFi and the WiMAX signals. Both the 2×2 and 4×4 are prototyped and are tested individually to obtain the simulation results [52].

The suggested antenna is capable of blocking the WiMAX and the WiFi signals, which are also capable of offering a gain value at the range of 3.5–6.2 dB also with a radiation efficiency in a range of more than 80%. A 4×4 UWB MIMO is used along with the RT Duroid substrate, using a dielectric constant material which has a thickness of about 0.787, which is liable to use in the wireless communication applications. A super-wide banded antenna has used here with a range of dimension in the rate of $32 \times 20 \times 0.8$ mm^3. These antennas are able to cover in a range of 2.9–30 GHz. The patch section used here uses with both the elliptical and with the circular shaped patches [53]. In order to reduce the economical and the industrial laybacks in the implementation of antenna use, the Phase-coding structures are introduces especially for the electromagnetic band gap resonator antennas. These make use of a light and a low fabricated material, which are not similar to the PCs. The suggested antenna model uses a metallic PCs, which are fabricated using the laser technology and are, evaluated for the ERA which resulted in the 19.42 dB as a peak gain value [54].

The incorporation of the stubs in the antenna, which are wide-banded, attached to a dual-stub with the defected ground structure uses in the Terahertz applications [55] by feeding a micro-strip line, which are stable in providing an impedance level of bandwidth in a range of 7.47 THz. Parametric analysis is evaluating the performance, which has a maximum gain value of 16.48 dB at an antenna range of 5.693 THz. The Rhombus shaped fractal antenna uses along with the stub, which are loaded and defected to the ground plane, uses in the wireless applications [56]. The stub introduced in the geometry of the antenna where the bandwidth of the antenna has been enhanced in a range of 17.53 GHz to a range of 19.25 GHz. the defected ground structure-which is based on the rectangular monopole antenna which is along with the 2×2 and also with the 4×4 MIMO antenna are attached along with the two slit notch and are placed in the optimum positions in order to enhance the impedance

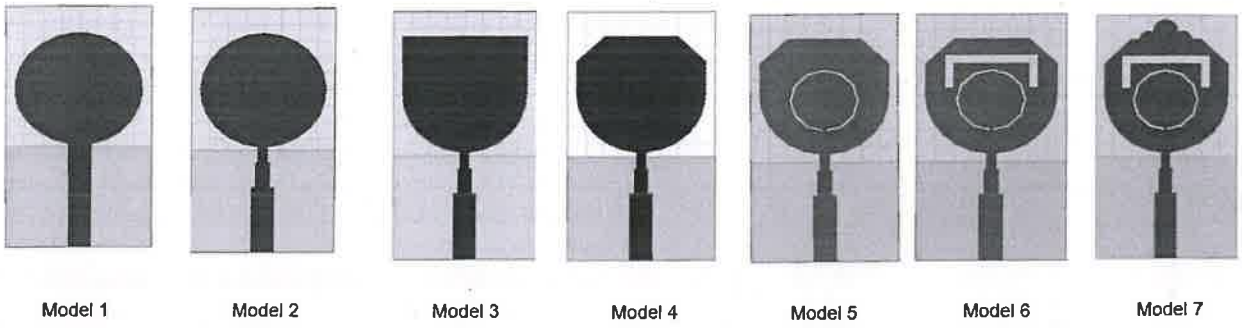

Fig. 1 Designing of single element antenna

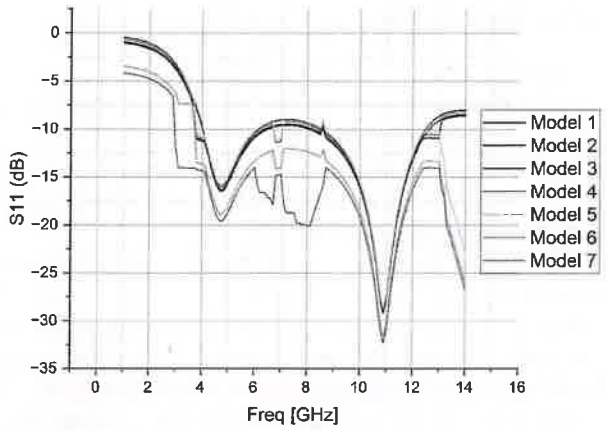

Fig. 2 S-Parameter of antenna (7 models)

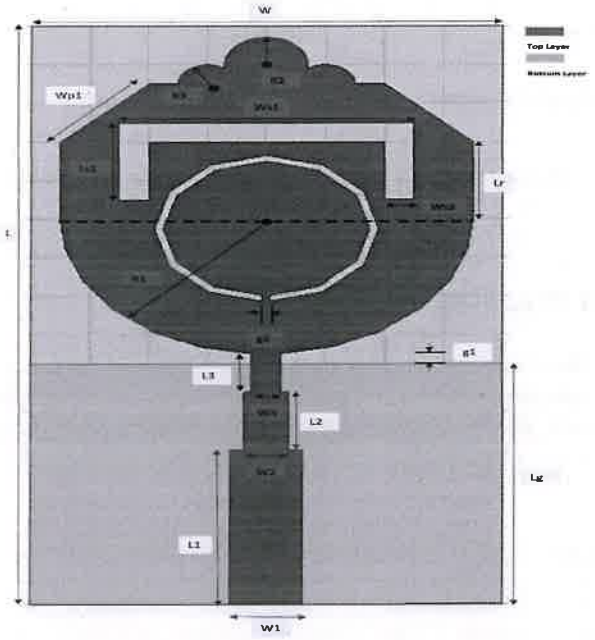

Fig. 3 Single element antenna

bandwidth. The radiator is also loaded with the U-shaped stub to enhance the matching with the respective antenna [57]. These can retain the transmission pulse, shape and can deliver a dispersion free form of communication. The performance has been based on the isolation and the envelope co-efficient values. The rectangular strip, which is engraved with the circular patch with the stub-shaped MIMO antenna, are replicated in the performance in a range of 1–25 GHz [58]. The suggested antenna has shown a maximum bandwidth of 5.49 GHz, and has observed with 5.65 GHz after the simulation of the respective antenna. A square-shaped wideband ultra-wide antenna are in a compact ground size which measures about 24×24 mm^2 which are constructed using a low cost FR-4 substrate [59]. A square shaped stub has been placed on the top of the radiating patch, which is optimized by the parametric analysis of the stub, which is square shaped. The impedance width which is obtained are in a range of < -10 dB. The optimal dimension of the stub has obtained in a range of 106.92% and in a frequency range of 3.53–11.64 GHz. IE3D simulation tool is used in the study to employ the process of designing and also for the simulation of the suggested antenna.

2.1 Problem identification

- The flexible antenna having a physical dimension of the range $39.8\times22\times0.1$ mm^3, offers a wide range of bandwidth, of 2.8lGHz. These are devoid to apply in the Stub 6 GHZ and in UWB applications which actually requires a bandwidth range of 3.1–10 GHz [60].
- To make the antenna to be more configurable, these antenna had to be embedded with active elements which ends up in high cost involvement and in the complex

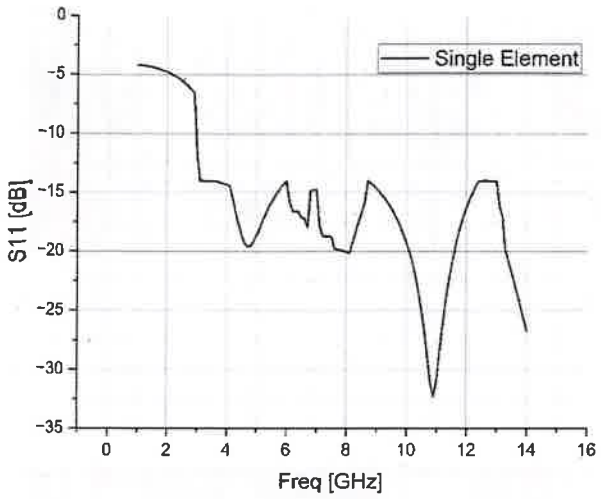

Fig. 4 S-Parameter of single element antenna

biasing of the network along with the control circuitry [61].

3 Proposed methodology

The stable connectivity in the network needsto maintain a proper configuration among the wireless mode of network. This is achieved using the appropriate and a suitable antenna, which have a control over network in an enhanced speed and relaibility of the network. The proposed study uses a 1×2 MIMO antenna where two antennas are separated at a distance of quarter wavelength distance, which behaves as a optimum distance for separation. If the distance of separation is too long form each other, there are increased chances of size of the antenna. Whereas if both the antennas are kept more closer, the chances of overlappping and the possibility of mutual coupling of the antenna are more. In order to reduce these chances of mutual coupling, several decopling structures can also be implemented. These MIMO antennas should be able to posses a lesser value of envelope such as correlation coefficient, less loss of capacity and with a high isolation loss value. This respective study uses a 1×2 UWB MIMO antenna which has been derived from the basic circular patch antenna.

Step 1: The circular patch antenna with a radius value of 7 mm are designed.

Step 2: To match the impedence, the stair-case like structure are adapted to the feed line.

Step 3: The first half of the circle is removed and are merged along with the rectangle which is in a size of 7 mm of length and 14 mm of width.

Step 4: Both the corners at the top of the rectangle are cut with a 45°

Step 5: A complementary split-ring resonator which is resembling a dodecagon shape, is patched into the antenna for the purpose of notching made at a levels of 5.6 GHz.

Step 6: To the patch section, an inverted U-shaped slot is introduced, which are centered at a range of 7.23 GHz.

Table 1 Different parameters and dimension of antenna

W1	2.87 mm	R1	7.1 mm	G1	0.6 mm	Lr	7.4 mm	L2	2.8 mm	Ws2	1 mm	W4	24 mm
W2	1.8 mm	R2	1.5 mm	G2	0.4 mm	L	30.5 mm	L3	1.8 mm	Ls1	4 mm	c	1.5 mm
W3	1.2 mm	R3	1 mm	Wp1	4.24 mm	W	16.3 mm	W5	12.5 mm	d	1 m		
L1	8.2 mm	Ws1	10 mm	Lg	12.3 mm	a	8 mm	Ws	42.2 mm	b	2.5 mm		

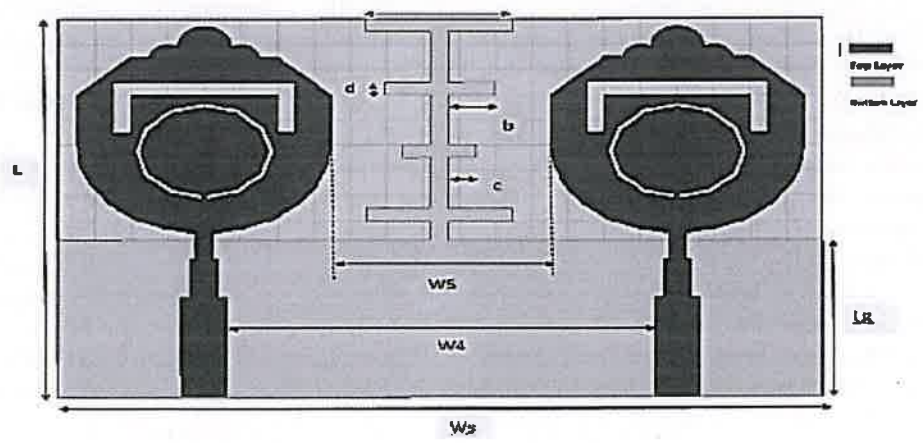

Fig. 5 Double element antenna construction

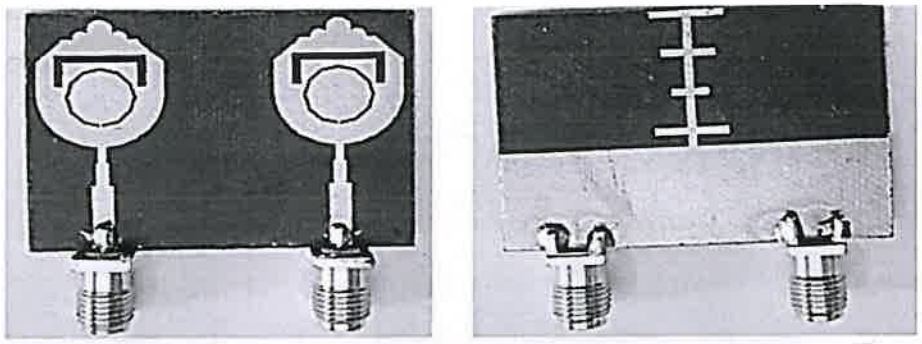

Fig. 6 Fabricated antenna elements (front and back view)

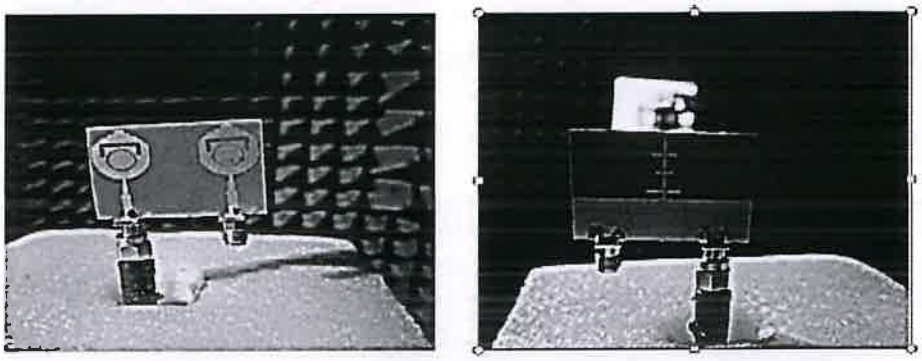

Fig. 7 Fabricated antenna connected to ancheoic chamber

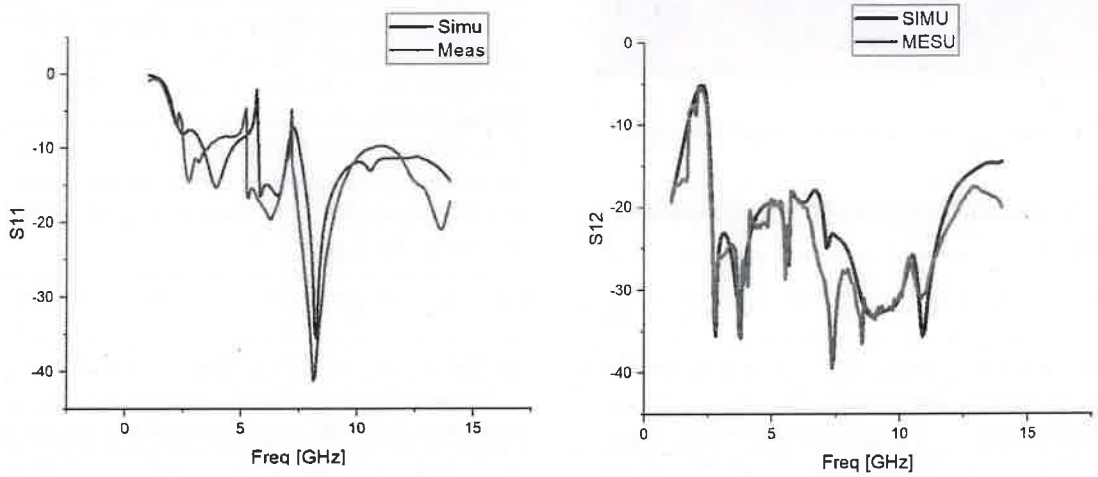

(i) S11 *(ii) S12*

Fig. 8 S-parameters of the proposed UWB-MIMO antenna

Step 7: To each of the patch section, three circles are introduced, in view of obtaining the UWB frequency of a operation.

Step 8: The Two-element antenna, UWB-MIMO which are at the same plane, in a spacing range of 13 mm. to reduce the couppling activity, the baseline shaped with four branched decoupled structure is introduced to the antenna. The isolation loss had achieved at a range of > -20 dB.

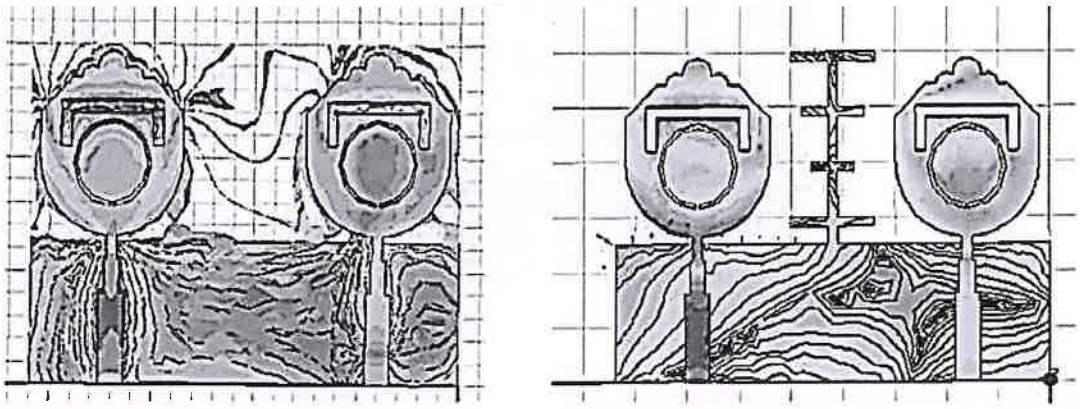

Fig. 9 flow of current in surface with and without stub attachment

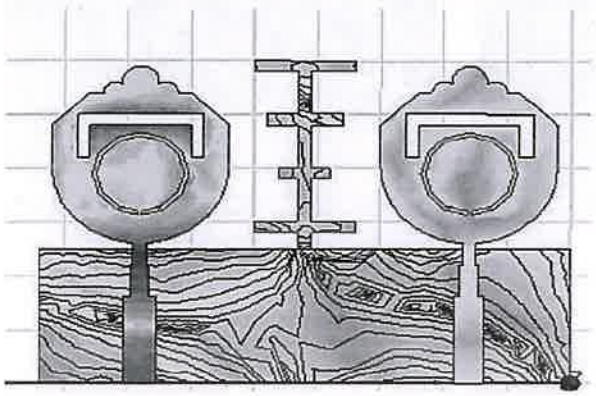

Fig. 10 distribution of surface current in proposed UWB-MIMO

3.1 The design and analysis of the singe element antenna

Initially the single element antenna are constructed where these patterns are relatively more wide and each of the element tends to provide lower values of directivity. These enlarged dimensions of single element antennas, are directive characteristics with increased size. They result in enlarged dimensions of the antennas. These array are identical but are not suitable for the practical nature of implementation. Figure 1 represents the basic designing of the spherical and pentagonal with the flower shaped antenna.

To overcome these drawbacks, the single element antennas are constructed with UWB-MIMO antenna, which are able to meet the next generation wireless communication networks. Embedding the multiple form of antennas into the same and single antenna system are one of the promising solution in enhancing the system channel capacity and the quality of communication link. But these are not adaptable for the small and hand-held devices, which are portable. In order to overcome these drawbacks, a two-element UWB MIMO is constructed which are suitable for the wireless form of communications. The S-parameter of Fig. 1 is shown below in Fig. 2.

The proposed study uses a single antenna element with the range of $30.5 \times 16.3 \text{x} 0.79$ mm^3. Figure 3 represents the single element antenna, which is constructed by the patch element along with the appropriatae MIMO antenna and notching. These antennas uses both the signal receiving and the transmission of signals. These can enhance the performance of the channels. The two-element array antenna consists of two U-shaped patch which are at similar dimensions where one antenna has a corporate feeding technique and have a quarter wave transform which is used in the task of impedance matching. These have two antennas, which are possible to connect simultaneously with two MIMO streams. The S-parameter of single element antenna is shown in Fig. 4.

The different parameters for antenna along with different dimensional values are listed in Table 1. Whereas, Fig. 5 depicts the designing and construction of double element antenna connected with the stub in it.

The proposed UWB-MIMO antenna is fabricated using the RT/Duroid 5880. Some of the PIFA based fabricated antennas uses in the wireless communication networks. Usually the antennas are fabricated using the ink jet technology and are evaluated. (Fig. 6)

These are connected to the ancheoic chamber which are isolated room and free from the Electromagnetic Waves and signals, which uses for testing of antenna. These chambers are able to simulate the antenna testing, if they are carried out in a outer space. The main purpose of using the ancheoic chamber are in supressing the EM wave energy which are in the form of echos. These can absorb the reflections of the respective waves which are within the chamber, instead of making them bounce off the

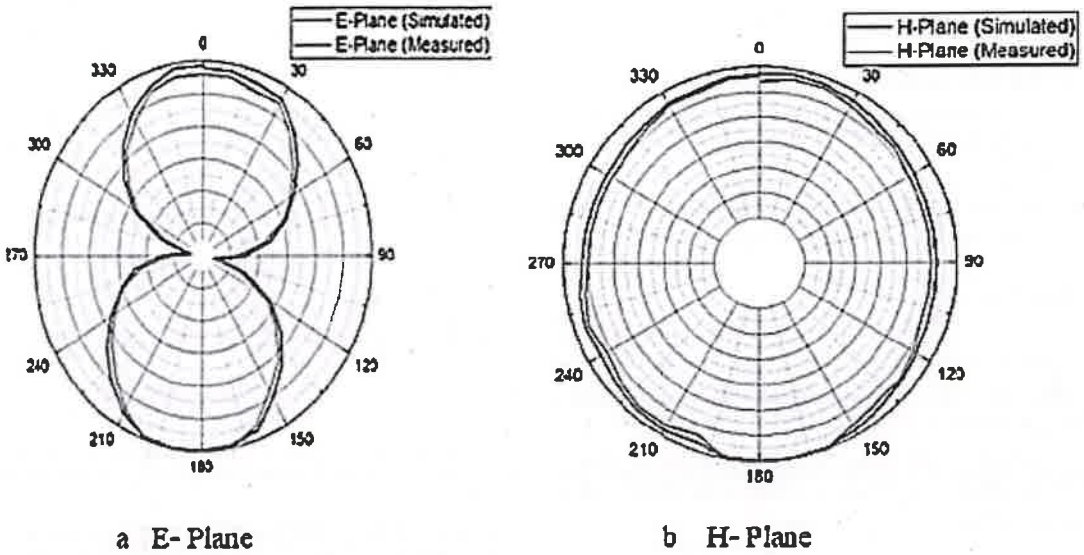

Fig. 11 Radiation pattern of the proposed UWB-MIMO antenna

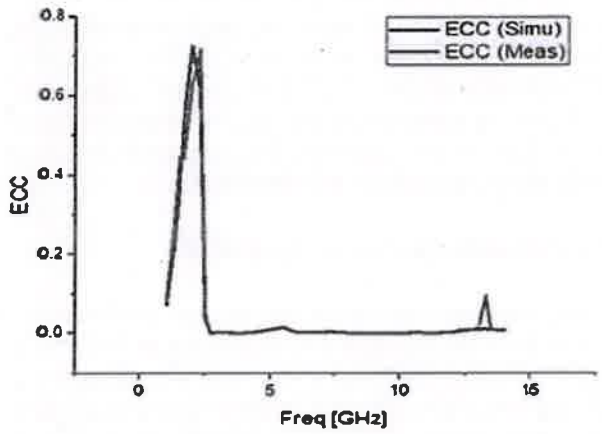

Fig. 12 ECC of the proposed UWB-MIMO antenna

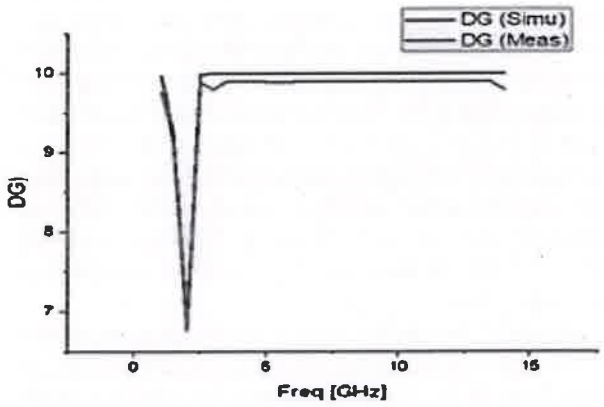

Fig. 13 DG of the proposed UWB-MIMO antenna

walls, whch results in forming echos. The Fig. 7 represent the antenna which are fabricated and are connected to the an ancheoic chamber.

4 Results and discussion

The study obtains appropriate results after the utilization of evaluation metric in analysing the performance of the suggested antenna model. The Agilent N5247A: A.09.90.02 vector network used in the characterisation of the proposed model, in view of evaluating its performance. These are also evaluated for its radiation properties, such as the patterns of radiation, peak gain are analysed in the ancheoic chamber.

Figure 8 (i) depicts S11 parameter of proposed UWB-MINO antenna simulation and the values are measured with the values of reflection co-efficient and plotted accordingly. The proposed antenna provides a wide band range of an operation from a 3.1 to 14 GHz. These are also calculated along with the notching frequencies which are at a values of 5.6 GHz to a 7.2 GHz. These antenna are able to block, the fast Wi-Fi band and also the C-band of the operation. These are the isolation loss which are simulated and are measured with the values which are plotted at the Fig. 8 (ii). Among the entire range of UWB the minimum value gained is about -20 dB. This is possible by using the Tree-like stub structure which is incorporated among the elements of antenna. There is a valid agreement which is noticed among the results which are simulated and are measured with the

S-parameters (S11 and S12) values. The stub covering the whole sub 6 GHz band.

The Fig. 9 illustrates the surface current distribution on the proposed UWB-MIMO antenna in two scenarios: These simulations are as follows:

(i) No stub attached to the central node and.
(ii) With stub attached as shown in Fig. 3.

Without the Stub:

Because the two radiating elements are coupled by the ground plane, the current flows between them and results into significant coupling. This coupling denotes the isolation of the elements and impacts the performance criteria such as Envelope Correlation Coefficient (ECC) and Diversity Gain (DG).

With the Stub:

The stub is incorporated into the design to provide a disruption to the direct coupling path, and instead channel the surface currents. It also improves the isolation by reducing the flows of unwanted currents towards the neighbouring components. This enhances critical specifications such as isolation loss (up to -20 dB) and diverseness of the system. It is also found that the stub used in the design also assists in achieving better control over the impedance matching and radiation efficiency of the antenna as can be seen from the measured S-parameters and simulated radiation pattern.

Figure 10 depicts the surface current flow in proposed UWB-MIMO antenna after the stub placement and the complete setup of the proposed antenna. The radiation pattern of antenna is the graphical representation of the radiation properties of the respective antenna as a function of space.

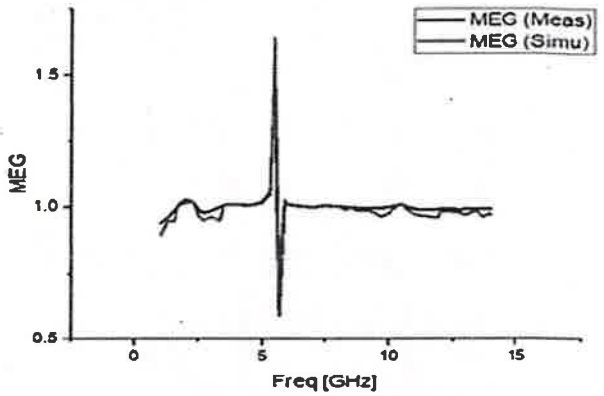

Fig. 15 obtained MEG values of the proposed UWB MIMO model

This is used in describing the function of antenna on how it radiates the energy or the electromagnetic wave into the space. These waves can be isotropic, omnidirectional or directional. This is important in antenna, which resembles the rate of power radiated per the unit solid angle. The proposed model exhibits an omni-directional radiation pattern. The two types of radiation pattern are the free space radiation and field radiation pattern. These radiation patterns are defined as the mathematical function, or a representation of the far field. This is represented using the $2D^2/\lambda$. Figure 11 represents the proposed UWB-MIMO antenna.

4.1 Performance metrics and analysis

The perfomance of the overall antenna, various characteristics of the MIMO antenna parameters such as ECC (Envelope Correlation Coefficient), the rate of diversity gain and also the total active reflection coefficient along with parameters such as mean effective gain, channel capacity loss are also evaluated. The initial parameter ECC is actually a crucial metric used in the calculation of mutual coupling which

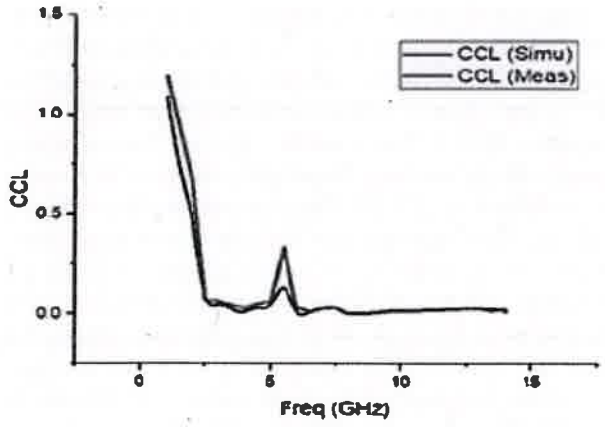

Fig. 14 CCL of the proposed UWB-MIMO model

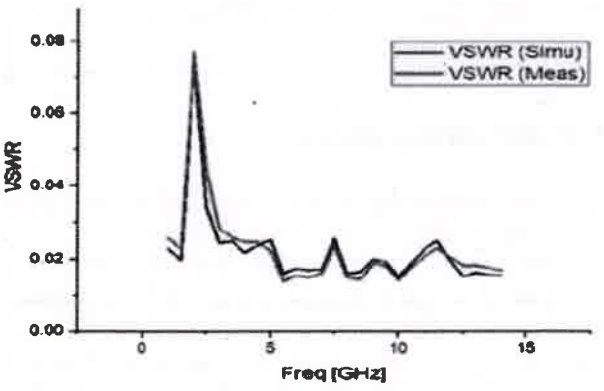

Fig. 16 obtained VSWR of the proposed MIMO antenna

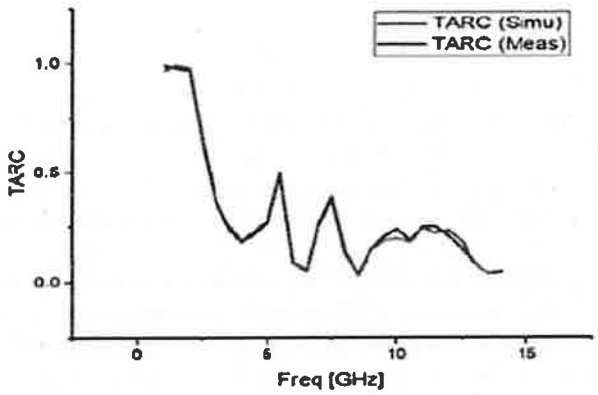

Fig. 17 TARC of the proposed MIMO antenna

occurs among two MIMO antenna elements. These depicts the values less than 0.5, for the condition of two-elelment antenna, and these ECC parameter are determined using the S parameter's relationship which is depicted in Eq. 1. It is used in the calculation of the diversity gain, which are observed at a range of 10 dB, throughout the entire range of operation. The proposed model of antenna, performs much better in the view of both the mutual food and also in terms of the diversity.

4.1.1 Envelope correlation coefficient

$$ECC = \frac{\left|S_{11}^{\times} S_{22} + S_{21}^{\times} + S_{22}\right|2}{\left(1 - \left|S_{11}^{2}\right| - \left|S_{21}^{2}\right|\right)\left(1 - \left|S_{22}^{2}\right| - \left|S_{22}^{2}\right|\right)} \quad (1)$$

Figure 12 represents the obtained Envelope Correlation coefficient of the proposed model.

4.1.2 Diversity gain

The Diversity Gain (DG) reduces the impact of the fading by the method of combining the antenna elements which can experience different fading points. These are characterised using the diversity order, the number of independent fading elements of the anternna. This is represented using the formula,

$$DG = 10\sqrt{1 - ECC^2} \quad (2)$$

Figure 13 represents the obtained Diversity Gain (DG) value, of the proposed UWB-MIMO antenna.

4.1.3 Channel capacity loss

This parameter is used in the evaluation of the losses which are occurred at the antenna, during the phase of transmission, which are represented using the bits/s/Hz. This is deived using a set of equation,

$$CCL = -log_2(\phi)^R \quad (3)$$

This is derived using the Eqs. (3a), (3b), (3c)

$$(\phi)^R = \begin{bmatrix} \phi_{11} & \phi_{12} \\ \phi_{21} & \phi_{22} \end{bmatrix} \quad (3a)$$

$$\phi_{11} = 1 - \left[|S_{11}|\right]2 - \left[|S_{12}|\right]2 \quad (3b)$$

$$\phi_{22} = 1 - \left[|S_{22}|\right]2 - \left[|S_{21}|\right]2 \quad (3c)$$

$$\phi_{12} = \left[|S_{22}|\right]2 - \left[|S_{21}|\right]2 \quad (3d)$$

$$\phi_{21} = -\left(S_{11} \times S_{12} \times S_{21} \times S_{22}\right) \quad (3e)$$

The CCL of the proposed model is depicted in Fig. 14. The obtained value of CCL is less than 0.1bits/S/GHz for the proposed model.

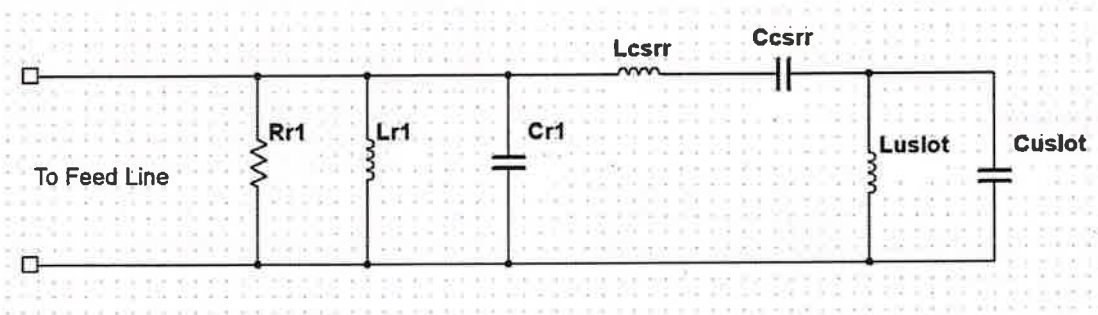

Fig. 18 Circuit model

4.1.4 Mean effective gain (MEG)

The value of MEG, is one of the vital parameter in the evaluation of the diversity of the perfomance in the proposed MIMO system. This is defined as the average rate of power which is received by the diversity antenna, relative to the power which is received by the isotropic antenna. This can also explain the rate of maximum amount of effectiveness to which the antenna can radiate the power which is reached to them by the use of transmittor, towards the desired target. This is calculated using the formula,

$$MEG = \frac{1}{2}[1 - [|S_{11}|]2 - [|S_{12}|]2] \quad (4)$$

These are derived from a couple of equation,

$$MEG2 = \frac{1}{2}1 - [|S_{21}|]2 - [|S_{22}|]2 \quad (4a)$$

$$MEG = \frac{MEG1}{MEG2} \quad (4b)$$

The obtained Mean Effective Gain value of the proposed UWB-MIMO antenna is clearly depicted in the value graph Fig. 15.

The values of VSWR, of the proposed MIMO antnna is seen in Fig. 16, which are at the values of 0.02 at the desired range of the complete operation.

4.1.5 Total active reflection coefficient (TARC)

The TARC represents the score, one of the important index for the evaluation of the MIMO antenna, which represents the square root of the total power which is reflected, divided by the total square root of the total amount of incident power which is represented in Fig. 17. This indicated that the outgoing power is the total unwanted amount of reflecte power. Figure 18 depicts the equivalent circuit of the analysis. This is calculaed using the formula,

$$TARC = \sqrt{\frac{(S_{11} + S_{12})2 + (S_{21} + S_{22})2}{\sqrt{2}}}/$$

5 Conclusion

The proposed two element UWB- MIMO antenna of size range of $30.5 \times 42.2 \times 0.79$ mm^3 uses sub 6 GHz and UWB applications, and used in providing enhanced rate of data. The proposed antenna is capable of blocking two ranges of frequencies, at a range of 5.6 GHz and 7.2 GHz. The dodecagon shaped CSRR is used to provide an enhanced notching at a range of 5.6 GHz. the inverted U-shaped slot which is used in the antenna has provided an increased range of notching at a range of 7.2 GHz. The decoupled structure is used for providing an increased rate of isolation loss, among the elements. The isolation loss has observed the desired and targeted frequency range is about > -20 dB. The proposed antenna has a low envelope correlation coefficient in a range of 0.01, and also a 10 dB range of DG and CCL in a range of 0.1bits/s/Hz. The simulation results depicts that the two-element UWB-MIMO antenna has resulted in the enhanced and increased isolation with higher gain rates which are relevant to use in Ultra Wide Band applications such as wireless automated monitors, camcorders and in the construction of portable media players.

Author contribution Credit Author Statement Santhakumar G, Contributes to Conceptualization, Data Curation, Formal Analysis, Methodology, Writing—Original draft. Dr. R. Muthukumar Contributes to Conceptualization, Data curation, Methodology, Project administration, supervision, validation.

Data availability No datasets were generated or analysed during the current study.

Declarations

Conflict of interests The authors declare no competing interests.

References

1. Mittal, D., Dhillon, A. S., Nag, A., & Bargota, R. (2018). High gain and highly directive microstrip patch antenna for radar and satellite communication. *Information and Communication Technology for Intelligent Systems: Proceedings of ICTIS, 2*(2019), 437–446.
2. Alsabah, M., Naser, M. A., Mahmmod, B. M., Abdulhussain, S. H., Eissa, M. R., Al-Baidhani, A., et al. (2021). 6G wireless communications networks: A comprehensive survey. *IEEE Access, 9*, 148191–148243.
3. Jiang, W., Han, B., Habibi, M. A., & Schotten, H. D. (2021). The road towards 6G: A comprehensive survey. *IEEE Open Journal of the Communications Society, 2*, 334–366.
4. Saad, W. (2021). 6G Wireless systems: challenges and opportunities. In *5G and Beyond: Fundamentals and Standards*, pp. 201–229.
5. Huang, T., Yang, W., Wu, J., Ma, J., Zhang, X., & Zhang, D. (2019). A survey on green 6G network: Architecture and technologies. *IEEE access, 7*, 175758–175768.
6. Ali, S., Sohail, M., Shah, S. B. H., Koundal, D., Hassan, M. A., Abdollahi, A., et al. (2021). New trends and advancement in next generation mobile wireless communication (6G): A survey. *Wireless Communications and Mobile Computing, 2021*, 1–14.
7. Wang, M., Lin, Y., Tian, Q., & Si, G. (2021). Transfer learning promotes 6G wireless communications: Recent advances and future challenges. *IEEE Transactions on Reliability, 70*, 790–807.
8. Chen, Y., Liu, W., Niu, Z., Feng, Z., Hu, Q., & Jiang, T. (2020). Pervasive intelligent endogenous 6G wireless systems: Prospects, theories and key technologies. *Digital communications and networks, 6*, 312–320.

9. Nadeem, Q. U. A., Kammoun, A., Chaaban, A., Debbah, M., & Alouini, M.-S. (2019). Intelligent reflecting surface assisted wireless communication: Modeling and channel estimation. *arXiv preprint* arXiv:1906.02360
10. Ali, S., Saad, W., Rajatheva, N., Chang, K., Steinbach, D., Sliwa, B., Wietfeld, C., Mei, K., Shiri, H., Zepernick, H. J., Chu, T. M. C., Ahmad, I., Huusko, J., Suutala, J., Bhadauria, S., Bhatia, V., Mitra, R., Amuru, S., Abbas, R.,... Malik, H. (2020). 6G white paper on machine learning in wireless communication networks. *arXiv preprint* arXiv:2004.13875
11. Al-Ansi, A., Al-Ansi, A. M., Muthanna, A., Elgendy, I. A., & Koucheryavy, A. (2021). Survey on intelligence edge computing in 6G: Characteristics, challenges, potential use cases, and market drivers. *Future Internet, 13*, 118.
12. Chowdhury, M. Z., Shahjalal, M., Hasan, M. K., & Jang, Y. M. (2019). The role of optical wireless communication technologies in 5G/6G and IoT solutions: Prospects, directions, and challenges. *Applied Sciences, 9*, 4367.
13. Vettikalladi, H., Sethi, W. T., Abas, A. F. B., Ko, W., Alkanhal, M. A., & Himdi, M. (2019). Sub-THz antenna for high-speed wireless communication systems. *International Journal of Antennas and Propagation, 2019*, 1–9.
14. Srivastava, H., & Tiwari, U. (2019). Design, simulation and analysis of rectangular and circular microstrip patch antenna for wireless applications. *International Journal of Recent Technology and Engineering (IJRTE), 8*, 2277–3878.
15. Malviya, L., Panigrahi, R. K., & Kartikeyan, M. (2020). *MIMO Antennas for Wireless Communication: Theory and Design.* CRC Press.
16. Tasolamprou, A. C., Pitilakis, A., Abadal, S., Tsilipakos, O., Timoneda, X., Taghvaee, H., et al. (2019). Exploration of intercell wireless millimeter-wave communication in the landscape of intelligent metasurfaces. *IEEE access, 7*, 122931–122948.
17. Chietera, F. P., Colella, R., & Catarinucci, L. (2021). Dielectric resonators antennas potential unleashed by 3D printing technology: A practical application in the IoT framework. *Electronics, 11*, 64.
18. Kumar, S., & Gupta, B. (2023). Design of compact textile MIMO with high isolation for wearable applications. *Wireless Personal Communications, 131*, 1–19.
19. Yang, W., Cheng, X., Guo, Z., Sun, Q., Wang, J., & Wang, C. (2023). Design, fabrication and applications of flexible RFID antennas based on printed electronic materials and technologies. *Journal of Materials Chemistry C, 11*, 406–425.
20. Whittaker, T., Zhang, S., Powell, A., Stevens, C. J., Vardaxoglou, J. Y. C., & Whittow, W. (2022). 3D printing materials and techniques for antennas and metamaterials: a survey of the latest advances. *IEEE Antennas and Propagation Magazine, 65*, 10–20.
21. Kaur, A., & Malik, P. K. (2021). Multiband elliptical patch fractal and defected ground structures microstrip patch antenna for wireless applications. *Progress In Electromagnetics Research B, 91*, 157–173.
22. Elechi, P., & Obi-Ijeoma, C. P. (2022). Performance analysis of an ultra-wide band (UWB) antenna for communication system. *Online Journal of Engineering Sciences, 2*, 1–12.
23. Khajawal, T., Rubani, Q., Rajawat, A., & Gupta, S. H. (2021). Performance analysis and optimization of band gap of terahertz antenna for WBAN applications. *Optik, 243*, 167387.
24. Hung, P. V., Dinh, N. Q., Yamada, Y., Michishita, N., & Islam, M. T. (2020). Parametric analysis of negative and positive refractive index lens antenna by ANSYS HFSS. *International Journal of Antennas and Propagation, 2020*, 1–11.
25. Saeidi, T., Ismail, I., Wen, W. P., Alhawari, A. R., & Mohammadi, A. (2019). Ultra-wideband antennas for wireless communication applications. *International Journal of Antennas and Propagation, 2019*, 1–25.
26. Xu, R., Gao, S., Izquierdo, B. S., Gu, C., Reynaert, P., Standaert, A., et al. (2020). A review of broadband low-cost and high-gain low-terahertz antennas for wireless communications applications. *Ieee Access, 8*, 57615–57629.
27. Saxena, R. S., Shrivastava, R., Muchhal, R., & Tiwari, R. (2020). Parametric Analysis and Design of 28GHz Microstrip Patch Antenna. *International Journal of Smart Vehicles and Smart Transportation (IJSVST), 3*, 38–58.
28. Al-Hiti, A. S. (2019). Design of rectangular microstrip patch antenna for WLAN and WiMAX applications. *ARPN Journal of Engineering and Applied Sciences, 14*, 433–438.
29. Shah, I., Hayat, S., Basir, A., Zada, M., Shah, S., & Ullah, S. (2019). Design and analysis of a hexa-band frequency reconfigurable antenna for wireless communication. *AEU-International Journal of Electronics and Communications, 98*, 80–88.
30. Ahmad, S., Ijaz, U., Naseer, S., Ghaffar, A., Qasim, M. A., Abrar, F., et al. (2022). A jug-shaped CPW-fed ultra-wideband printed monopole antenna for wireless communications networks. *Applied Sciences, 12*, 821.
31. Patel, R., Desai, A., Upadhyaya, T., Nguyen, T. K., Kaushal, H., & Dhasarathan, V. (2021). Meandered low profile multiband antenna for wireless communication applications. *Wireless Networks, 27*, 1–12.
32. Kundu, S. (2019). Experimental study of a printed ultra-wideband modified circular monopole antenna. *Microwave and Optical Technology Letters, 61*, 1388–1393.
33. AmramBengio, E., Senic, D., Taylor, L. W., Headrick, R. J., King, M., Chen, P., et al. (2019). Carbon nanotube thin film patch antennas for wireless communications. *Applied Physics Letters, 114*, 203102.
34. Ahmad, Z., Kabir, A., & Bukhari, S. S. H. (2021). A novel compact stair-shaped multiband fractal antenna for wireless communication systems. *Journal of Electrical Engineering, 72*, 306–314.
35. Soothar, P., Wang, H., Muneer, B., Dayo, Z. A., & Chowdhry, B. S. (2021). A broadband high gain tapered slot antenna for underwater communication in microwave band. *Wireless Personal Communications, 116*, 1025–1042.
36. Azim, R., Meaze, A. M. H., Affandi, A., Alam, M. M., Aktar, R., Mia, M. S., et al. (2021). A multi-slotted antenna for LTE/5G Sub-6 GHz wireless communication applications. *International Journal of Microwave and Wireless Technologies, 13*, 486–496.
37. Dayo, Z. A., Cao, Q., Wang, Y., Soothar, P., Khoso, I. A., Shah, G., et al. (2021). A compact high gain multiband bowtie slot antenna with miniaturized triangular shaped metallic ground plane. *The Applied Computational Electromagnetics Society Journal (ACES), 36*, 935–945.
38. Li, J., Zhang, X., Wang, Z., Chen, X., Chen, J., Li, Y., et al. (2019). Dual-band eight-antenna array design for MIMO applications in 5G mobile terminals. *IEEE Access, 7*, 71636–71644.
39. Qiu, B., Xia, Y., & Li, Y. (2022). Gain-enhanced wideband circularly polarized antenna with a non-uniform metamaterial reflector. *The Applied Computational Electromagnetics Society Journal (ACES), 37*, 281–286.
40. Rajanna, P. K. T., Rudramuni, K., & Kandasamy, K. (2019). A high-gain circularly polarized antenna using zero-index metamaterial. *IEEE Antennas and Wireless Propagation Letters, 18*, 1129–1133.
41. Liu, Y., Huang, Y. X., Liu, Z. W., Cai, S. T., Xiong, X. M., & Guo, J. (2020). A new broadband circularly polarized antenna with a single-layer metasurface. *International Journal of RF and Microwave Computer-Aided Engineering, 30*, e22226.
42. Tran, H. H., Bui, C. D., Nguyen-Trong, N., & Nguyen, T. K. (2021). A wideband non-uniform metasurface-based circularly polarized reconfigurable antenna. *IEEE Access, 9*, 42325–42332.

43. Soothar, P., Wang, H., Xu, C., Dayo, Z. A., Muneer, B., & Kanwar, K. (2020). A compact broadband and high gain tapered slot antenna with stripline feeding network for H, X, Ku and K band applications. *International Journal of Advanced Computer Science and Applications, 11*, 239–244.
44. Azim, R., Alam, T., Paul, L. C., Aktar, R., Meaze, A. M. H., & Islam ,M. T. (2020) Low profile multi-slotted patch antenna for lower 5G application. In *2020 IEEE Region 10 Symposium (TENSYMP)*, pp. 366–369.
45. Tahseen, H. U., Yang, L., & Catarinucci, L. (2022). A triple band dual-polarized multi-slotted antenna array for base station applications. *Wireless Networks, 28*, 1475–1487.
46. Paul, L. C., Jim, M. T. R., Rani, T., Ankan, S. S. A., Das, S. C., & Saha, H. K. (2022). A Π-shaped slotted patch antenna with a partial ground structure for lower 5G/WiFi/WiMAX applications. *Heliyon, 8*, e10934.
47. Malik, P. K., & Singh, M. (2019). Multiple bandwidth design of micro strip antenna for future wireless communication. *International Journal of Recent Technology and Engineering, 8*, 5135–5138.
48. Sharma, M., Kumar, R., Kaur, P., Dhasarathan, V., & Nguyen, T. K. (2022). Design and analysis of on-demand reconfigurable WiMAX/WLAN high isolation 2× 2 MIMO antenna oriented adjacent/orthogonally for imaging applications in UWB-X band. *International Journal of RF and Microwave Computer-Aided Engineering, 32*, e22928.
49. Hadda, L., Sharma, M., Gupta, N., Kumar, S., & Singh, A. K. (2021). On-demand reconfigurable WiMAX/WLAN UWB-X band high isolation 2× 2 MIMO antenna for imaging applications. *IETE Journal of Research, 69*, 1–13.
50. Dhasarathan, V., Nguyen, T. K., Sharma, M., Patel, S. K., Mittal, S. K., & Pandian, M. T. (2020). Design, analysis and characterization of four port multiple-input-multiple-output UWB-X band antenna with band rejection ability for wireless network applications. *Wireless Networks, 26*, 4287–4302.
51. Bhattacharya, A., Roy, B., Caldeirinha, R. F., & Bhattacharjee, A. K. (2019). Low-profile, extremely wideband, dual-band-notched MIMO antenna for UWB applications. *International Journal of Microwave and Wireless Technologies, 11*, 719–728.
52. Sharma, M. (2020). Design and analysis of MIMO antenna with high isolation and dual notched band characteristics for wireless applications. *Wireless Personal Communications, 112*, 1587–1599.
53. Sharma, M., Dhasarathan, V., Patel, S. K., & Nguyen, T. K. (2020). An ultra-compact four-port 4× 4 superwideband MIMO antenna including mitigation of dual notched bands characteristics designed for wireless network applications. *AEU-International Journal of Electronics and Communications, 123*, 153332.
54. Lalbakhsh, A., Afzal, M. U., Esselle, K. P., & Smith, S. L. (2020). Low-cost nonuniform metallic lattice for rectifying aperture near-field of electromagnetic bandgap resonator antennas. *IEEE Transactions on Antennas and Propagation, 68*, 3328–3335.
55. Das, V., & Rawat, S. (2021). Modified rectangular planar antenna with stubs and defected ground structure for THz applications. *Optik, 242*, 167292.
56. Sharma, N., & Bhatia, S. S. (2021). Ultra-wideband fractal antenna using rhombus shaped patch with stub loaded defected ground plane: Design and measurement. *AEU-International Journal of Electronics and Communications, 131*, 153604.
57. Hasan, M. N., Chu, S., & Bashir, S. (2019). A DGS monopole antenna loaded with U-shape stub for UWB MIMO applications. *Microwave and optical technology letters, 61*, 2141–2149.
58. Almawgani, A. H., & Sorathiya, V. (2023). Rectangular strip engraved circular patch and connected corrugated stub-based MIMO antenna for Wi-Fi/5G/WiMAX/satellite communication applications. *Applied Physics A, 129*, 200.
59. Verma, R. K., & Srivastava, D. (2021). Bandwidth improvement of stub loaded compact ultra-wideband microstrip patch antenna for C/X-band applications. *Wireless Personal Communications, 120*, 185–202.
60. Saha, T. K., Knaus, T. N., Khosla, A., & Sekhar, P. K. (2022). A CPW-fed flexible UWB antenna for IoT applications. *Microsystem Technologies, 28*, 5–11.
61. OjaroudiParchin, N., JahanbakhshBasherlou, H., Al-Yasir, Y. I., Abd-Alhameed, R. A., Abdulkhaleq, A. M., & Noras, J. M. (2019). Recent developments of reconfigurable antennas for current and future wireless communication systems. *Electronics, 8*, 128.

Mr. G. Santhakumar presently working as Assistant Professor, Department of ECE in Sri Krishna College of Technology, Coimbatore, India. He received his B.E degree in Electronics and Communication engineering from the Anna University in 2010 and received his M.E in Communication system in 2012 from Anna University and Pursuing Ph.D in Information and Communication Engineering at Anna University, Chennai. His main research interests include mm Wave antennas, 5G antennas and Communication.

Dr. R. Muthukumar presently working as Associate professor, Department of EEE in Erode Sengunthar Engineering College, Erode, India. He received his B.E Degree in Electrical and Electronics Engg. from CIT, Coimbatore, M.E., in Power Systems Engg. From GCT, Coimbatore and completed Ph.D in Power System Engineering at Anna University, Chennai, in 2014. He has published more than eighteen international journals and has fifteen International/National conference publications. His research interest includes power system planning, voltage stability analysis and application of evolutionary algorithms to power system optimization.